Evaluation of Optimization Algorithms for Fracture Parameter Calibration in Spent Nuclear Fuel Cladding with Reoriented Hydrides

Seyeon Kim [a*], Sanghoon Lee [a]
[a] *Department of Mechanical Engineering, Keimyung Univ., Daegu 42601, Korea*
[*] *Corresponding author: shlee1222@kmu.ac.kr*

Keywords : spent nuclear fuel, hydride reorientation, pinch load, finite element analysis, parameter calibration

1. Introduction

Maintaining the structural integrity of spent nuclear fuel (SNF) cladding under transport and handling conditions is essential for safe and economic management of SNF. The U.S. Nuclear Regulatory Commission (NRC) has raised concerns that hydride reorientation may compromise cladding integrity under hypothetical accident conditions, particularly in horizontal drop tests where pinch loads can induce longitudinal tearing (Mode-III failure). The Ring Compression Test (RCT) is commonly used to evaluate fracture resistance and shows that radial hydrides act as primary crack pathways and that the Zr/hydride interface has the lowest crack resistance. To evaluate fracture behavior, an RCT simulation model has been developed using a ductile damage model [1], but parameter calibration is challenging due to the complex parameter space and limited experimental data. To address this, a metamodeling framework was developed to calibrate fracture parameters from RCT data. Two optimization algorithms, GSA and GA, were applied for parameter calibration and their execution time, accuracy and practicality were compared.

2. Methods and Results

2.1 Finite Element Model

The finite element model was constructed from the microscopic images of the irradiated cladding. A pixel-based finite element model was constructed by separating the hydride, zirconium matrix, and interface. The image segmentation method was based on morphology operations [1].

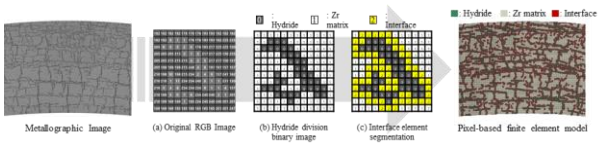

Fig. 1. Microstructural finite element modeling process using metallographic image.

In RCT, maximum tensile stress and crack initiation were observed on the outer walls at the 3 o'clock and 9 o'clock positions and on the inner walls at the 12 o'clock and 6 o'clock positions. Accordingly, a microstructural finite element model constructed from metallographic image was applied at the main crack initiation positions. Other regions were simplified as a homogeneous material without hydrides for numerical efficiency. The analysis was performed using the four-node plane strain element (CPE4R) in ABAQUS.

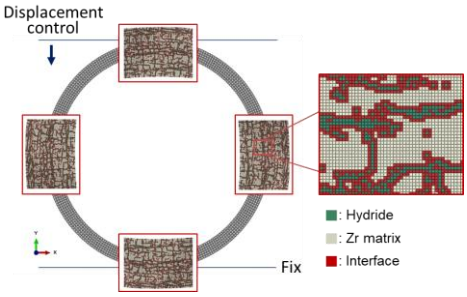

Fig. 2. Finite element model for RCT simulation.

2.2 Material Property

The Young's modulus of the Zr matrix and δ-hydrides in the microstructural finite element model were defined based on literature data [2-10]. The material properties of the simplified regions were derived from the specifications of the cladding specimen, RCT load-displacement data [11-14].

Table I: Young's modulus and yield stress of microstructural finite element model and simplified region.

	Young's modulus	Yield stress
Zr matrix	85 GPa	684 MPa
Hydride	95 GPa	1410 MPa
Interface	95 GPa	905 MPa
Simplified region	99 GPa	859 MPa

2.3 Damage mechanics model

We propose a microstructure crack propagation analysis method based on Continuum Damage Mechanics (CDM) to simulate the fracture behavior of hydrides, the zirconium matrix, and the Zr/hydride interface. A ductile damage model in ABAQUS was used to simulate crack initiation and propagation in these three regions, considering the deformation of the cladding.

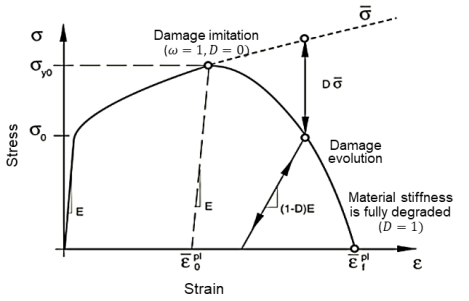

Fig. 3. Stress-strain curve with progressive damage degradation.

The key parameters of the ductile damage model are summarized in the Table II. In RCT, the strain rate can be neglected under quasi-static conditions; therefore, damage initiation is primarily influenced by stress triaxiality. Previous studies have shown that the fracture strains at three representative triaxiality levels—pure shear (η=0.00), uniaxial tension (η=0.33), and plane strain (η=0.58)— are sufficient to accurately simulate the cladding failure behavior under RCT conditions [1].

Table II: Major fracture parameters of ductile damage model for cladding with precipitates.

Factors	Fracture parameters	
θ_1	G_f	Fracture energy
θ_2	$\bar{\varepsilon}^{pl}_{0,\ \eta:0}$	Equivalent plastic strain at damage initiation ($\eta = 0$, pure shear)
θ_3	$\bar{\varepsilon}^{pl}_{0,\ \eta:0.3:}$	Equivalent plastic strain at damage initiation ($\eta = 0.33$, uniaxial tension)
θ_4	$\bar{\varepsilon}^{pl}_{0,\ \eta:0.5}$	Equivalent plastic strain at damage initiation ($\eta = 0.58$, plane strain)

According to the study by Chan et al [2], the Zr/hydride interface has the lowest failure stress and displacement. Therefore, the interface region is assumed to have the greatest influence on crack initiation and we will calibrate the main fracture parameters in this region. Furthermore, the initial load drop in the force-displacement curve of the RCT, which indicates crack initiation, can be reasonably attributed to the fracture characteristics of the Zr/hydride interface.

2.4 Metamodel

To replace the computationally expensive RCT simulation model for parameter calibration, a metamodel was constructed. The Kriging metamodel was selected as the metamodeling technique, and training data was generated based on the Optimal Latin Hypercube (OLH) design, which was then used for metamodeling.

2.3 Optimization Formulation

This study focuses on the first load drop in the RCT curve, the fracture parameters of the Zr/hydride interface were specifically fine-tuned. The optimization for the fracture parameters calibration was formulated as in equation (1):

(1) Find $\boldsymbol{\theta} = [\theta_1, \theta_2, \theta_3, \theta_4]$ such that
Minimize $f(\boldsymbol{\theta}) = |CL_E - CL_S| + |CD_E - CD_S|$
Subject to $\boldsymbol{\theta}_{lb} \leq \boldsymbol{\theta} \leq \boldsymbol{\theta}_{ub}$

where θ_{1-4} represent the fracture parameters of the interface in Table I, and $\boldsymbol{\theta}$ is the vector of fracture parameters, CL and CD are the crack initiation load and displacement, respectively. The subscripts E and S denote the experimental and simulation data, respectively, and $\boldsymbol{\theta}_{lb}$ and $\boldsymbol{\theta}_{ub}$ are the lower and upper bounds of the parameters.

2.5 Optimization Algorithms

The objective function for fracture parameter calibration is highly nonlinear, which makes the optimization process prone to converge to local optima. Therefore, in this study, fracture parameters were calibrated using the Global Search Algorithm (GSA) and the Genetic Algorithm (GA) to increase the probability of finding the global optimum, and their performances were compared.

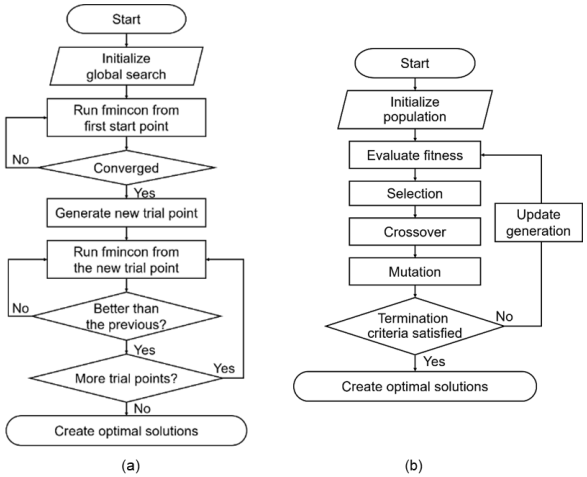

Fig. 4. Optimization process: (a) Global Search Algorithm, (b) Genetic Algorithm.

2.6 Result and Comparison

The optimized interfacial fracture parameters obtained from GSA and GA were applied to the RCT simulation model, and both showed good agreement with the experimental data. The crack initiation load and displacement from both optimizations were within 0.96% and 0.82% of the experimental values, respectively, confirming the high prediction accuracy. While both models predicted similar crack propagation along the radial hydride interface, slight differences in crack growth patterns were observed due to variations in θ_2 and θ_3. Both algorithms showed similar optimization

performance, with GSA completing in 18.19 seconds and GA in 18.62 seconds.

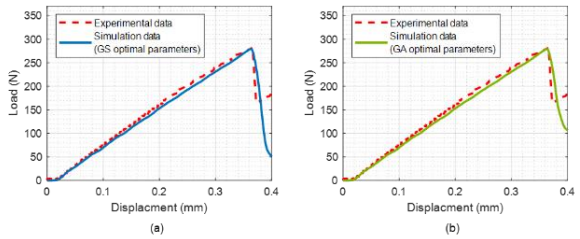

Fig. 5. Comparison of load-displacement curves between experimental and simulation results: (a) simulation using GSA-optimized parameters, (b) simulation using GA-optimized parameters.

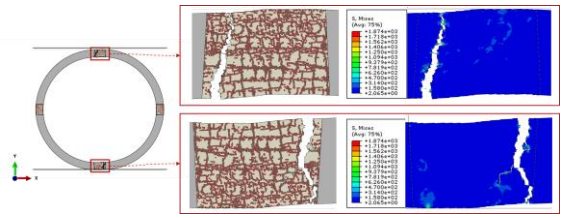

Fig. 6. Simulation result of a GSA-optimized parameter set.

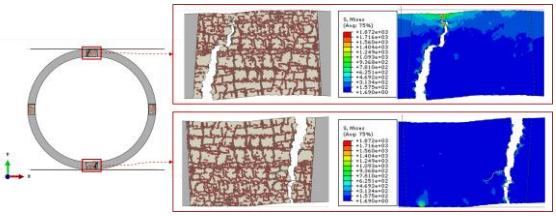

Fig. 7. Simulation result of a GA-optimized parameter set.

3. Conclusions

In this study, fracture parameters for cladding with reoriented hydrides under pinch load were calibrated using an RCT simulation model and a metamodeling approach with GSA and GA. Key parameters were calibrated and high prediction accuracy was achieved with errors of 0.96% and 0.82% for crack initiation load and displacement, respectively. Both algorithms produced identical crack initiation predictions, with slight differences in crack propagation due to θ_2 and θ_3. The Kriging metamodel significantly reduced computational cost while improving optimization efficiency. Future research will refine additional fracture parameters and incorporate hydride morphology uncertainties for improved failure simulations.

REFERENCES

[1] S. Kim and S. Lee, Methodology for numerical evaluation of fracture resistance under pinch loading of spent nuclear fuel cladding containing reoriented hydrides, Nuclear Engineering and Technology, Vol. 56, no. 6, pp. 1975–1988, Jun. 2024.
[2] M. P. Puls, S.-Q. Shi, and J. Rabier, Experimental studies of mechanical properties of solid zirconium hydrides, Journal of nuclear materials, Vol. 336, no. 1, pp. 73–80, 2005.
[3] A. Rico, M. A. Martin-Rengel, J. Ruiz-Hervias, J. Rodriguez, and F. J. Gomez-Sanchez, Nanoindentation measurements of the mechanical properties of zirconium matrix and hydrides in unirradiated pre-hydrided nuclear fuel cladding, Journal of nuclear materials, Vol. 452, no. 1–3, pp. 69–76, 2014.
[4] S. Yamanaka et al., Thermal and mechanical properties of zirconium hydride, J Alloys Compd, Vol. 293, pp. 23–29, 1999.
[5] M. Kuroda, K. Yoshioka, S. Yamanaka, H. Anada, F. Nagase, and H. Uetsuka, Influence of precipitated hydride on the fracture behavior of zircaloy fuel cladding tube, J Nucl Sci Technol, Vol. 37, no. 8, pp. 670–675, 2000.
[6] C. Evans, Micromechanisms and micromechanics of Zircaloy-4, Imperial college, London, United Kingdom, 2014.
[7] W. Zhu, R. Wang, G. Shu, P. Wu, and H. Xiao, First-principles study of different polymorphs of crystalline zirconium hydride, The Journal of Physical Chemistry C, Vol. 114, no. 50, pp. 22361–22368, 2010.
[8] P. F. Weck, E. Kim, V. Tikare, and J. A. Mitchell, Mechanical properties of zirconium alloys and zirconium hydrides predicted from density functional perturbation theory, Dalton Transactions, Vol. 44, no. 43, pp. 18769–18779, 2015.
[9] S. Suman, M. K. Khan, M. Pathak, and R. N. Singh, Investigation of elevated-temperature mechanical properties of δ-hydride precipitate in Zircaloy-4 fuel cladding tubes using nanoindentation, J Alloys Compd, Vol. 726, pp. 107–113, 2017.
[10] H. Chan, S. G. Roberts, and J. Gong, Micro-scale fracture experiments on zirconium hydrides and phase boundaries, Journal of Nuclear Materials, Vol. 475, pp. 105–112, 2016.
[11] J. A. Deruntz and P. G. Hodge, Crushing of a tube between rigid plates, Journal of Applied Mechanics, Transactions ASME, Vol. 30, no. 3, pp. 391–395, 1960.
[12] T. Y. Reddy and S. R. Reid, On obtaining material properties from the ring compression test, Nuclear Engineering and Design, Vol. 52, no. 2, pp. 257–263, 1979.
[13] M. Nemat-Alla, Reproducing hoop stress–strain behavior for tubular material using lateral compression test, Int J Mech Sci, Vol. 45, no. 4, pp. 605–621, Apr. 2003.
[14] B. Garrison, Y. Yan, and S. TerMaath, Determining failure properties of as-received and hydrided unirradiated Zircaloy-4 from ring compression tests, Eng Fail Anal, Vol. 125, p. 105362, Jul. 2021.